

See discussions, stats, and author profiles for this publication at: <https://www.researchgate.net/publication/271589570>

Systematic Evaluation of Mathematical Methods and Numerical Schemes for Modeling PCM-enhanced Building Enclosure

ARTICLE in ENERGY AND BUILDINGS · JANUARY 2015

Impact Factor: 2.88 · DOI: 10.1016/j.enbuild.2015.01.044

CITATIONS

3

READS

129

2 AUTHORS, INCLUDING:

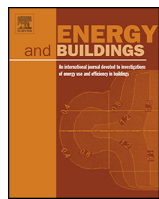


[Saleh N.J. Al-Saadi](#)

Sultan Qaboos University

20 PUBLICATIONS 64 CITATIONS

[SEE PROFILE](#)



Systematic evaluation of mathematical methods and numerical schemes for modeling PCM-enhanced building enclosure



Saleh Nasser Al-Saadi ^{a,*}, Zhiqiang (John) Zhai ^{b,1}

^a Department of Civil and Architectural Engineering, Sultan Qaboos University, PO Box 33, Muscat Postal code 123, Oman

^b Department of Civil, Environmental, and Architectural Engineering, University of Colorado at Boulder, Boulder, CO 80309-0428, USA

ARTICLE INFO

Article history:

Received 14 September 2014

Received in revised form 13 January 2015

Accepted 21 January 2015

Available online 31 January 2015

Keywords:

PCM modeling

Mathematical methods

Numerical schemes

MATLAB/SIMULINK

Building enclosure

ABSTRACT

Latent heat storage using phase change material (PCM) has become one of the most viable solutions to mediate the climatic deficiency of light weight structures. Instead of expensive field tests, computational modeling can be utilized to evaluate its technical and economic feasibility. This study presents the calculation procedure for eight potential numerical models/schemes implemented in MATLAB/SIMULINK environment. A linearized enthalpy method with hybrid correction scheme is proposed as an improvement to the existing numerical schemes. The models have been validated and further verified against a well-known building simulation program "EnergyPlus". The models have been analyzed for their computational efficiency and prediction accuracy. Some models are found sensitive to PCM's melting range, for example heat capacity method, but less sensitive to the latent heat. For all models, the time step should be small for accurate results. The iterative and the hybrid correction schemes are found computationally efficient and less sensitive to variations of PCM properties. In addition, a maximum time step of 15 min can be used without significant numerical error or changes in computational time. Hence, these two schemes can potentially be implemented into whole building simulation tools for modeling PCMs instead of existing slow and unstable numerical algorithms.

© 2015 Elsevier B.V. All rights reserved.

1. Introduction

The comparison of various energy storage solutions reveals that latent heat storage using PCMs is probably one of the most viable solutions at the current development stage. Due to its ability of storing significant thermal energy within a small volume, PCM appears one of most promising technologies for developing energy efficient buildings, particularly useful to reduce the inherited climatic deficiency in light weight buildings. To quantify the technical and economic feasibility of using PCM for building applications, computational models of PCM-enhanced systems are highly desired. Computational modeling offers inexpensive alternative to solve phase change heat transfer problems when compared to field studies for analyzing, optimizing and fine-tuning designs. For envelope systems with constant properties, heat transfer mechanisms can be readily solved using variety of approaches [1,2]. However, when

PCMs are utilized, special treatment is necessary to account for dynamic heat storage and release.

Analytical solutions for heat transfer with phase change are difficult to derive. Very few analytical solutions for simple cases are available in closed form for phase change problems [3–5]. Therefore, approximate numerical solutions are usually used to handle this class of problems. Recent studies have outlined the mathematical modeling of phase change materials for building applications [6–12]. Others have particularly described the mathematical forms, numerical models and validation efforts for building's enclosures [13–27]. However, a group of experts among the International Energy Agency's (IEA) Annex 23 team members concluded, based on their comprehensive review on the PCM modeling, that the confidence in PCM models is too low to use for future building's behavior [28]. Moreover, the reviewed models are not tested in a very stringent or exhaustive way.

Integrated PCMs models into whole building simulation programs are as important as individual stand-alone models. The whole building simulation programs are essential design tools for architects and engineers to evaluate new concepts and test advanced technologies that may improve the energy and thermal performance of buildings. Several building simulation tools are listed at the U.S. Department of Energy (DOE) web directory [29].

* Corresponding author. Tel.: +968 24142697; fax: +968 24141331.

E-mail addresses: salsaadi@squ.edu.om (S.N. Al-Saadi), John.Zhai@colorado.edu (Z. Zhai).

¹ Tel.: +1 303 4924699; fax: +1 303 4927317.

Nomenclature

<i>a</i>	matrix coefficient
<i>C</i>	storage coefficient
<i>c</i>	specific heat capacity
<i>f</i>	fluid fraction of PCM
<i>h</i>	enthalpy
<i>k</i>	thermal conductivity
<i>L</i>	latent heat of fusion
<i>S</i>	source term
<i>T</i>	Temperature
<i>T_s</i>	solidus temperature (i.e. $T_m - \epsilon$)
<i>T_l</i>	liquidus temperature (i.e. $T_m + \epsilon$)
<i>t</i>	time
<i>n</i>	number of data points
<i>x</i>	space distance

Greek symbols

ϵ	half range temperature
ϕ	variable
Γ_ϕ	diffusion coefficient
ω	under-relaxation factor
ρ	density

Subscripts

avg	average
e	east node
eff	effective
<i>l</i>	liquid state
<i>m</i>	melting
<i>p</i>	point node
<i>s</i>	solid state
w	west node

Superscripts

<i>A</i>	apparent
<i>m</i>	indicates an iteration step
<i>n</i>	indicates a time step

The most twenty common detailed energy simulation programs that are considered accurate and capable of handling the dynamic behavior of building and its systems are reviewed by Crawley et al. [30]. Few whole building simulation programs can handle the thermal performance of building envelope with phase change materials such as EnergyPlus [31], TRNSYS [32], ESP-r [33], and BSim [34]. Majority of PCM models integrated into whole building simulation programs are based on the heat capacity method [12]. The method has been implemented with small time steps for accurate predictions [34–36]. Hence, it becomes necessary to reduce the typical one hour time step to a very small time step (i.e., in order of minutes) to achieve acceptable level of accuracy. For one year thermal performance evaluation, building simulation programs become computationally inefficient since iterative methods are used in each time step. Additionally, the convergence may not be achieved due to numerical instability especially when PCM enters or leaves the phase change region. This is vital since design decisions may be based on inaccurate results. With all constraints and limitations above, none of whole building simulation programs are currently implementing efficient mathematical models that are quick, accurate and numerically stable at realistic time step. It becomes important to thoroughly investigate different mathematical models of PCMs with various numerical approaches for possible considerations into whole building simulation programs. Several challenges including accuracy,

numerical stability and computational efficiency, are however confronted when selecting a specific scheme and a suitable numerical solver.

In light of the above reviews, the motivation for this study is the great desire to determine appropriate models, associated schemes and solvers that can be used for a quick yet accurate simulation of PCMs at realistic time step. This particular need is pronounced when the algorithms are to be integrated into whole building simulation programs that perform yearly simulations at hourly and sub-hourly time steps. Therefore, the objective of this study is to investigate common numerical schemes and the related algorithms that can be used to solve the nonlinearity with PCMs in conduction-dominated heat transfer problems similar to those that are common in building applications. In particular, it focuses on modeling PCM-enhanced building enclosures for potential implementation into whole building simulation tools.

2. Mathematical methods, numerical schemes and discretization for modeling phase change problems

Phase change problems can be solved using fixed grid method [37–39], deforming grid method [4], or hybrid method [40]. The fixed grid method is simple compared to the others, most versatile, convenient, adaptable and easily-programmable [4]. Therefore, it is considered in this study. Using fixed grid method, several mathematical models are used to simulate heat transfer associated with phase change: enthalpy method [41–45], heat capacity method [46–49], temperature transforming model [50–53], heat source method [45,54–57], or other methods [37,38,58]. Three common mathematical models, based on enthalpy method, heat capacity method, and heat source method, are selected for further evaluation.

For conduction-dominated heat transfer problems, the governing equation of phase change can be written in a general form as:

$$C \frac{\partial \phi}{\partial t} = \frac{\partial}{\partial x} \left(\Gamma_\phi \frac{\partial \phi}{\partial x} \right) + S \quad (1)$$

Table 1 briefly summarizes the features and mathematical coefficients used to generate the three mathematical forms for modeling phase change materials.

The numerical models and schemes considered under this study are based on general assumptions. Majority of building simulation programs are based on one dimensional heat transfer model and therefore the same is assumed in this work. A fully implicit time stepping scheme is utilized for all models since it is unconditionally stable regardless of the time step. The spatial discretization is based on the finite volume method and the harmonic average suggested by Patankar [59] for materials conductivity is used. Typical grid points for a system of wall layers using finite volume method are illustrated in Fig. 1.

The convergence is declared using this relationship: error = $|\sum(T - T_{\text{new}})/\sum(T_{\text{new}})|$, where T is a vector of nodes temperature from previous iteration and T_{new} is the new results [60]. Under-relaxation is implemented for some models. For example, Voller et al. [39] recommended a value between 0.5 and 0.7 for heat source

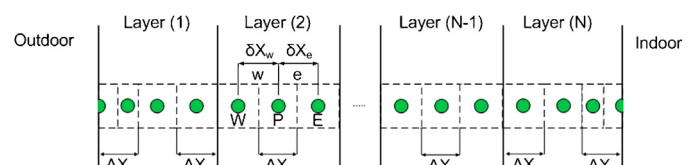


Fig. 1. Grid points location for numerical models using finite volume method.

Table 1

Mathematical formulation used for Phase Change Problems.

Mathematical methods for PCMs modeling	Coefficients				Main feature
	C	ϕ	Γ_ϕ	S	
Enthalpy method	ρ	h	k/C_p	0	Enthalpy term accounts for sensible and latent heat
Heat capacity method	$\rho^*C^A(T)$	T	k	0	Heat capacity term accounts for both sensible and latent heat
Heat source method	ρ^*C_{avg}	T	k	$-\rho \times L \times (\partial f_l / \partial t)$	Latent heat is treated as a source term

method. Their study indicated that a factor in this range provides efficient convergence for both one- and two-dimensional cases. For all models developed in this section, the hysteresis and sub-cooling are not considered. Although they are important, studies found that they are either negligible or less important in building envelope [61,62]. The enthalpy–temperature (h –T) performance curve shown in Fig. 2 is a basic piece of information that is necessary when solving latent heat problems.

For many PCMs, minimal design information pertained to the thermal characteristics such as melting temperature; melting range and latent heat are provided by manufacturers. Although the models described in this study can be solved with detailed h –T performance curve, a simplified h –T performance curve defined by four points is assumed. Other assumptions pertained to specific model is outlined when the scheme is described. In addition, boundary conditions will be described under each section as appropriate. The following sections outline the numerical discretization and calculation procedure using these three general methods.

2.1. Enthalpy method

Using coefficients from Table 1 and utilizing Eq. (1), the general heat transfer model based on enthalpy method can be discretized as follows:

$$\rho \frac{h_p^{n+1} - h_p^n}{\Delta t} = k_w \frac{T_w^{n+1} - T_p^{n+1}}{\Delta X \times \delta X_w} + k_e \frac{T_e^{n+1} - T_p^{n+1}}{\Delta X \times \delta X_e} \quad (2)$$

Collecting and rearranging terms, Eq. (2) becomes:

$$h_p^{n+1} = h_p^n + a_w \times T_w^{n+1} + a_p \times T_p^{n+1} + a_e \times T_e^{n+1} \quad (3)$$

$$\text{where } a_w = \frac{k_w \times \Delta t}{\rho \times \Delta X \times \delta X_w}, \quad a_e = \frac{k_e \times \Delta t}{\rho \times \Delta X \times \delta X_e}, \quad a_p = -(a_w + a_e)$$

The discretized Eq. (3) is nonlinear since both h_p^{n+1} and T^{n+1} are unknown at this time step. Therefore, linearization is used to solve the equation using techniques proposed by Patankar [59]. The h_p^{n+1}

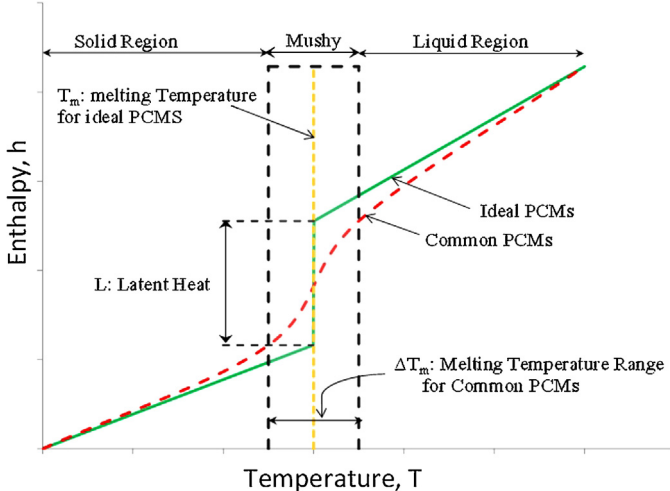


Fig. 2. Enthalpy–temperature (h –T) performance curve for ideal and common PCMs

term can be expanded using Taylor series first order approximation. At iterative level, the h_p^{n+1} term can be written as:

$$h_p^{n+1,m+1} = h_p^{n+1,m} + C(T)^{n+1,m} \times (T_p^{n+1,m+1} - T_p^{n+1,m}) \quad (4)$$

The subscript “ $n+1$ ” represents the current time step, “ n ” means the previous time step, “ $m+1$ ” is the current iteration and “ m ” is the previous iteration. At the start of simulation, the temperature fields are based on guess values. Hence, $C(T)^{n+1,m}$ (tentative values that will be updated at the beginning of the iteration) can be found using [63]:

$$C(T) = \begin{cases} C_s & T \leq T_{m-} \\ \frac{C_s + C_l}{2} + \frac{L}{2\epsilon} & T_{m-} < T < T_{m+} \\ C_l & T \geq T_{m+} \end{cases} \quad (5)$$

When Eq. (4) is substituted into Eq. (3) and after rearrangement and collecting terms, the following linear discretized equation is derived:

$$\begin{aligned} a_w^{n+1,m} \times T_w^{n+1,m+1} + a_p^{n+1,m} \times T_p^{n+1,m+1} + a_e^{n+1,m} \times T_e^{n+1,m+1} \\ = R^{n+1,m} \end{aligned} \quad (6)$$

where

$$a_w^{n+1,m} = -\frac{k_w \times \Delta t}{\rho \times \Delta X \times \delta X_w}, \quad a_e^{n+1,m} = -\frac{k_e \times \Delta t}{\rho \times \Delta X \times \delta X_e}$$

$$\begin{aligned} a_p^{n+1,m} &= (C(T)^{n+1,m} + a_w^{n+1,m} + a_e^{n+1,m}) \\ R^{n+1,m} &= (h_p^n - h_p^{n+1,m} + C(T)^{n+1,m} \times T_p^{n+1,m}). \end{aligned}$$

The discretized Eq. (6) can be solved using different schemes as will be described in the following sections.

2.1.1. Generalized enthalpy method

When no further numerical techniques are adopted, Eq. (6) can be written in a general point form as follows:

$$\begin{aligned} T_p^{n+1,m+1} &= \frac{1}{a_p^{n+1,m}} \times \left[R^{n+1,m} - \sum a_w^{n+1,m} \times T_w^{n+1,m+1} \right. \\ &\quad \left. - \sum a_e^{n+1,m} \times T_e^{n+1,m} \right] \end{aligned} \quad (7)$$

Eq. (7) can be solved for $T^{n+1,m+1}$ using Gauss–Seidel algorithm. Once the temperature field is determined, the node enthalpies are calculated using Eq. (4). In order to avoid a numerical instability, under-relaxation factor is applied. The new node enthalpies are subsequently used in the next iteration. The iteration process continues until convergence is achieved. The iteration process is not complemented with a correction step for this scheme compared to other schemes in the next sections.

2.1.2. Iterative correction scheme

Following the generalized enthalpy method procedure above, the iterative correction scheme developed by Swaminathan and

Voller [42] can be written in a matrix format which is solved by a direct solver. Eq. (6) can then be written as:

$$[A]^{n+1,m} \times T^{n+1,m+1} = R^{n+1,m} \quad (8)$$

This equation can be solved for $T^{n+1,m+1}$ using Tri-diagonal matrix algorithm (TDMA). Once the temperature field is determined, the node enthalpies are updated using Eq. (4). At this iteration instant, the enthalpy is known and therefore the temperature field is corrected to be in consistent with enthalpy temperature performance curve using the following relationship [63]:

$$T_p = \begin{cases} \frac{h_p}{C_s}, & h_p \leq C_s \times (T_m - \epsilon) \\ \frac{h_p + [(C_l - C_s)/2] + (L/(2 \times \epsilon)) \times (T_m - \epsilon)}{[(C_l + C_s)/2] + (L/(2 \times \epsilon))}, & C_s \times (T_m - \epsilon) < h_p < C_l \times (T_m + \epsilon) + L \\ \frac{h_p - (C_s - C_l) \times T_m - L}{C_l}, & h_p \geq C_l \times (T_m + \epsilon) + L \end{cases}$$

The iteration process in this prediction-correction cycle continues until convergence is achieved.

2.1.3. Non-iterative correction scheme

The non-iterative scheme proposed by Pham [49] is similar to the previous one except that no iterations are attempted and therefore no convergence criterion is specified. The matrix coefficients are based on temperature results from previous time step. For this reason, the scheme can be considered as a semi-implicit. Using TDMA algorithm, the temperature field is determined when Eq. (8) is solved. The enthalpy is calculated using Eq. (4) and subsequently the temperature field is corrected using Eq. (9) before proceeding to the next time step. No further iterations are performed in a time step. The matrix coefficients are updated for the next time step based on the corrected temperature field.

2.1.4. Hybrid correction scheme

In building simulations, energy systems are modeled on hourly bases using typical metrological weather data. When PCMs are incorporated into building systems, a sub-hourly simulation is required to accurately capture the latent heat liberation. Therefore, a quick but energy conservative approach is highly demanded. Previous sections have outlined potential quick schemes that are commonly used to solve latent heat problems with few that fulfil the unique requirement of building simulations; the iterative correction scheme developed by Swaminathan and Voller [42] and non-iterative scheme proposed by Pham [49]. The prediction-correction cycles are demonstrated using h - T curve shown in Fig. 3. Fig. 3 (a) shows the iterative correction scheme numerically progresses through solving the latent heat problem in two consecutive time steps when the PCM is going through solidification process. At first time step, the guess values of both temperature and enthalpy values (liquid state: point (a) in Fig. 3(a)) are based on previous time step. Using this guess point for determining the matrix coefficients, the scheme predicts the new nodal temperatures (point (b) in Fig. 3(a)) and subsequently calculates the corresponding nodal enthalpy. Since the enthalpy is the same for any point on a horizontal line, the temperature is corrected using the h - T curve (point (c) on Fig. 3(a)). This new enthalpy and temperature values are used as guess values for next iteration. The scheme iterates going through the same process until convergence is achieved at this time step (point (e) on Fig. 3(a)). For the next time step, the numerical solution follows the line a', b', c', d', e' in Fig. 3(a) as it did in the first time step until convergence is achieved. The number of iterations depends on the convergence limit. Although the slope is the same if a PCM doesn't change a state, it is observed that there are unnecessary iterations for this scheme. On the other hand, Fig. 3(b) demonstrates

how the non-iterative correction scheme solves the latent heat problem. The same calculation procedure as that for the iterative correction scheme is adopted except that the solution is reached in a single correction step. The matrix coefficients are based on previous time step solutions and therefore there is a risk of reaching inaccurate results. This risk is not substantial when a node is on a single state but signifies as the node's state progresses from one state (say a liquid) to a different state (say a mushy). The correction step adopted by both schemes makes the numerical solution fast since direct solvers can be utilized. Iteration process, on the other

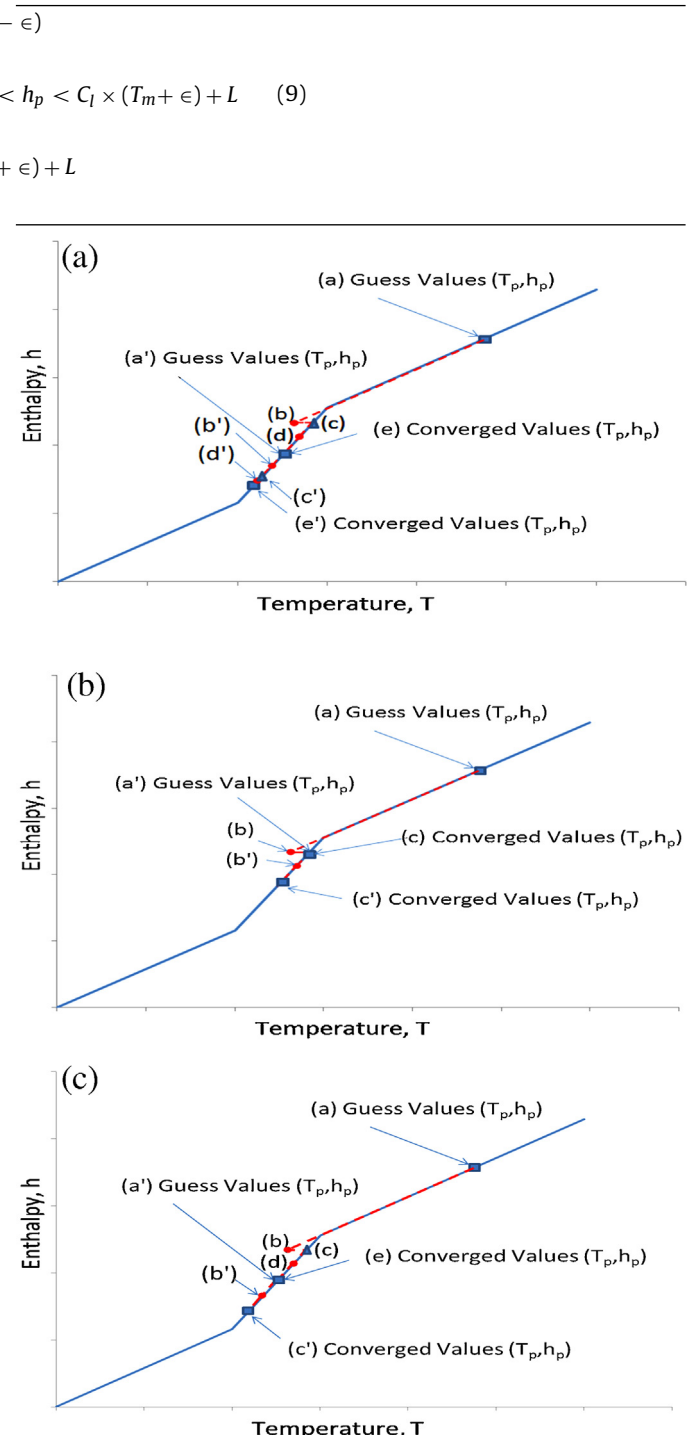


Fig. 3. Advances of numerical solutions using correction schemes during two consecutive time steps: (a) Iterative correction scheme, (b) Non-iterative correction scheme, (c) Hybrid correction scheme.

hand, makes the solution robust and rigorous since the energy is balanced at each time step. The new scheme should therefore be based on these two features for modeling phase change materials in future generations of building simulation tools.

Fig. 3(c) shows the concept of the proposed improvement for a new hybrid scheme that combines the features of both schemes. The hybrid correction scheme iterates the solution when at least one PCM's node enters or leaves a state. Since the slope on the simplified $h-T$ curve doesn't change during a state, several iterations can be eliminated during the time period. Therefore, a checking step is introduced to determine the current slope for each node using Eq. (5). If the slope is constant (i.e. the apparent specific heat is the same for the nodes during a time step), then the solution advances to the next time step otherwise iterate the solution until the slope is constant between iterations. Therefore, the number of iterations decreases when compared to the iterative correction scheme since it mimics the non-iterative correction scheme feature. On the other hand, the scheme iterates the solution when a node enters or leaves a state, making it conservative as the case with the iterative correction scheme. Therefore, this approach switches between the iterative and non-iterative correction schemes based on the state of the node.

2.2. Heat capacity method

The heat capacity term in the governing equation imitates the effect of enthalpy (sensible and latent heat) by increasing the heat capacity value during the phase changing stage. Based on **Table 1** and Eq. (1), the governing equation is written in terms of a single unknown variable with a non-linear coefficient (i.e. the apparent heat capacity). In a similar fashion to the enthalpy method when the heat equation is discretized, a point form can be written as follows:

$$T_p^{n+1,m+1} = \frac{1}{a_p^{n+1,m}} \times \left[R^{n+1,m} - \sum a_w^{n+1,m} \times T_w^{n+1,m+1} - \sum a_e^{n+1,m} \times T_e^{n+1,m} \right] \quad (10)$$

where

$$a_w^{n+1,m} = -\frac{k_w \times \Delta t}{\rho \times \Delta X \times \delta X_w}, \quad a_e^{n+1,m} = -\frac{k_e \times \Delta t}{\rho \times \Delta X \times \delta X_e}$$

$$a_p^{n+1,m} = (C^A(T) + a_w^{n+1,m} + a_e^{n+1,m}), \quad R^{n+1,m} = \left(C^{A^{n+1,m}} \times T_p^n \right)$$

When using Gauss-Seidel algorithm, the solution sweeps from west to east node. Therefore, the solution for the point node will be based on the updated value of west node but still use an old value from previous iteration for the east node. The solution iterates until convergence is achieved. The apparent heat capacity term can be evaluated numerically using the temporal averaging proposed by Morgan [64] using the following equation:

$$C^{A^{n+1,m}} = \frac{\Delta h}{\Delta T} = \frac{h^{n+1,m} - h^n}{T^{n+1,m} - T^n + 10^{-6}} \quad (11)$$

In order to avoid the division by zero in Eq. (11), a value of “ 10^{-6} ” is added to the denominator. Alternatively, the discretized equation (10) can be solved using TDMA algorithm [18]. It must be mentioned, however, that the solution might not converge at higher time step and small time step is necessary when TDMA is used.

2.3. Heat source method

In a common approach proposed by Swaminathan and Voller [39,56] to deal with PCMs in mushy regions, the heat equation using the heat source method from **Table 1** and Eq. (1) can be written as:

$$\rho \times C_{avg} \times \frac{\partial T}{\partial t} = \frac{\partial}{\partial x} \left(k \frac{\partial T}{\partial x} \right) - \rho \times L \times \frac{\partial f_l}{\partial t} \quad (12)$$

Liquid fraction “ f_l ” can be evaluated using the following liquid fraction-temperature relationship [65]:

$$f_l = \begin{cases} 1, & \text{if } T > T_L \\ \frac{(T - T_s)}{(T_L - T_s)}, & \text{if } T_s \leq T \leq T_L \\ 0, & \text{if } T < T_s \end{cases} \quad (13)$$

Similar to the Heat capacity method, when Eq. (12) is discretized using the fully implicit scheme, it becomes:

$$T_p^{n+1,m+1} = \frac{1}{a_p^{n+1,m}} \times \left[R^{n+1,m} - \sum a_w^{n+1,m} \times T_w^{n+1,m+1} - \sum a_e^{n+1,m} \times T_e^{n+1,m} \right] \quad (14)$$

where

$$a_w^{n+1,m} = -\frac{k_w \times \Delta t}{\rho \times \Delta X \times \delta X_w}, \quad a_e^{n+1,m} = -\frac{k_e \times \Delta t}{\rho \times \Delta X \times \delta X_e},$$

$$a_p^{n+1,m} = \left(C_{avg} + L \times \left. \frac{df}{dT} \right|_{fm} + a_w^{n+1,m} + a_e^{n+1,m} \right)$$

$$R^{n+1,m} = C_{avg} \times T_p^n + L \times \left(f_{l,p}^n - f_{l,p}^{n+1,m} + \left. \frac{df}{dT} \right|_{fm} \times T_p^{n+1,m} \right)$$

The term $\left. df/dT \right|_{fm}$ is evaluated based on previous two iterations using the numerical approximation approach:

$$\left. \frac{df}{dT} \right|_{fm} = \begin{cases} \frac{f_{l,p}^{n+1,m} - f_{l,p}^{n+1,m-1}}{T_p^{n+1,m} - T_p^{n+1,m-1} + 10^{-6}}, & \text{if } 0 < f_{l,p}^{n+1,m} < 1 \\ 0, & \text{if } f_{l,p}^{n+1,m} = 1 \text{ or } f_{l,p}^{n+1,m} = 0 \end{cases} \quad (15)$$

In order to avoid division by zero in Eq. (15), a value of “ 10^{-6} ” is added to the denominator. After solving for temperature field at all nodes, the liquid fraction is updated which is a key to this scheme using the following equation:

$$f_{l,p}^{n+1,m+1} = f_{l,p}^{n+1,m} + \omega \times \text{SLOPE} \times (T_p^{n+1,m+1} - T_p^{n+1,m}) \quad (16)$$

where

$$\text{SLOPE} = \begin{cases} \left. \frac{df}{dT} \right|_{fm}, & \text{if } 0 < f_{l,p}^{n+1,m} < 1 \\ \frac{C_{avg}}{L}, & \text{if } f_{l,p}^{n+1,m} = 1 \text{ or } f_{l,p}^{n+1,m} = 0 \end{cases}$$

ω : under-relaxation factor (0.5–0.7) [39].

Practically, the update is done for all nodes including those that don't undertake phase change. Therefore, an under-shoot/overshoot correction is applied to ensure that fluid fraction takes values between 0 and 1 using the following relation:

$$f_{l,p} = \begin{cases} 0, & \text{if } f_{l,p}^{n+1,m+1} < 0 \\ 1, & \text{if } f_{l,p}^{n+1,m+1} > 1 \end{cases} \quad (17)$$

Table 2

Characteristics of the tested numerical methods and schemes.

Method	Solver	Scheme Identification	Correction Step	Under-relaxation
Enthalpy method (EM)	G-S	Generic (EM_Generic_GS)	No	Yes (=0.8)
	TDMA	Iterative Correction Scheme (EM_ICS_TDMA)	Yes	No
	TDMA	Hybrid Correction Scheme (EM_HCS_TDMA)	Yes	No
	TDMA	Non-Iterative Correction Scheme (EM_NIC_TDMA)	Yes	No
Heat capacity method (HCM)	TDMA	HCM_TDMA	No	No
Heat source method (HSM)	G-S	HSM_GS	No	No
	TDMA	HSM_TDMA	Yes	Yes (=0.5)
	G-S	HSM_GS	Yes	Yes (=0.5)

G-S: Gauss-Seidel, TDMA: Tri-diagonal matrix algorithm.

Before proceeding to the next iteration, the temperature field must also be corrected for the case when the nodes are in the mushy region using the following relationship:

$$T_p^{*,n+1,m+1} = \begin{cases} T_p^{n+1,m+1}, & \text{if } f_{l,p} < 0 \text{ or } f_{l,p} > 1 \\ T_S + f_{l,p} \times (T_L - T_S), & \text{if } 0 < f_{l,p} < 1 \end{cases} \quad (18)$$

Alternatively, the temperature can be corrected using Eq. (9) after determining the enthalpy using the following relationship:

$$h_p^{n+1,m+1} = C_{avg} \times T_p^{n+1,m+1} + f_{1,p}^{n+1,m+1} \times L \quad (19)$$

Then, the iteration process is repeated until convergence is attained. When arranged in a matrix format, the discretized equation (14) can also be solved using TDMA algorithm.

2.4. Calculation procedure

According to the previous sections, a wide selection of numerical schemes and solvers can be utilized for solving phase change problems. Table 2 summarizes the characteristics of the tested numerical methods, schemes, and solvers. Although not optimized, under-relaxation factor is used for schemes that have shown numerical instabilities. Fig. 4 illustrates the calculation procedure of all models when implemented into MATLAB/SIMULINK environment.

3. Verification and validation of numerical models

Buildings are exposed to environmental conditions such as outside air temperature, wind, and solar radiations. The exterior envelope exchanges heat with the environment via convection heat transfer, short wave radiation and long wave radiation. Since these phenomena are nonlinear, analytical solutions are difficult to

EM: Enthalpy Method
HCM: Heat Capacity Method
HSM: Heat Source Method
ICS: Iterative Correction Scheme
NIC: Non-Iterative Correction Scheme
HCS: Hybrid Correction Scheme
TDMA: Tri-Diagonal Matrix Algorithm

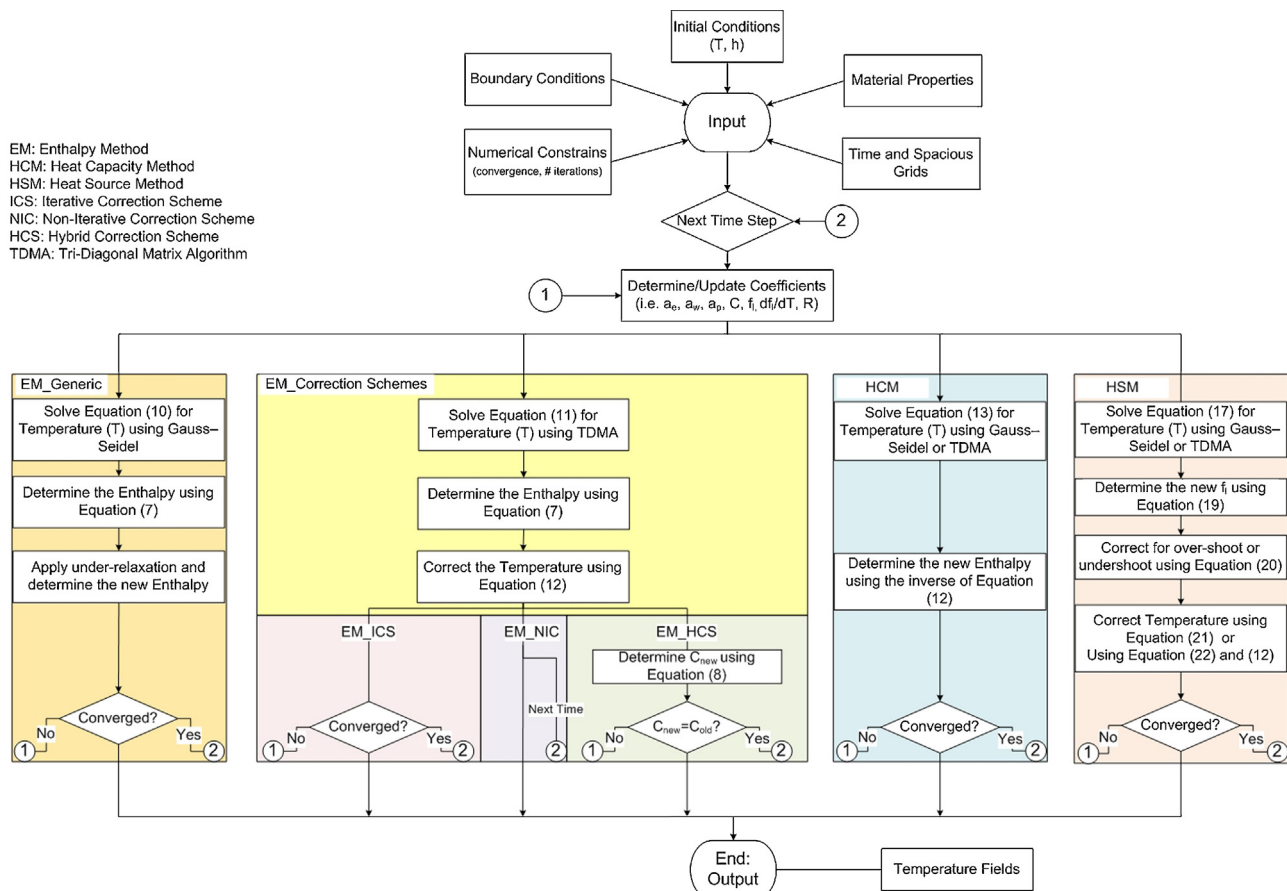


Fig. 4. Flow chart of the calculation procedure implemented for all models in MATLAB/SIMULINK environment.

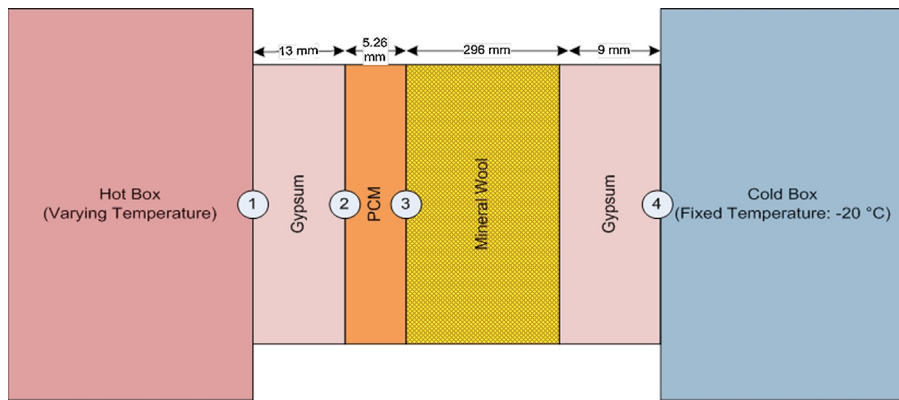


Fig. 5. Environmental test chamber with wall configuration and temperature sensors location.

Table 3

Thermal properties of materials used in the tested PCM wall assembly.

Material	Thermal Conductivity [W/(m K)]	Density [kg/m ³]	Thickness [m]	Heat Capacity [J/(kg K)]	Latent heat [kJ/kg]	Ref.
Gypsum	0.21	700	0.009 at hot side 0.013 at cold side	1000		[67]
PCM, (DuPont Energain)	0.18	856	0.00526	836.8	Refer to Fig. 6 (a)	[35,66,67]
Mineral wool	0.037	16	0.296	1030		[67]

develop. Experimental results from lab cells or field studies can be used to validate the numerical models. The accuracy of the results is however dependent on instrumentation used. In addition, a software-software comparison can also be utilized for verification. These two approaches have been used to validate and verify the models developed in this study.

3.1. Validation using experimental results

In order to quantify the benefits of PCMs under dynamic environmental conditions, lab tests, field studies or actual implementation in large scale buildings are considered. The results from these studies can be used as bases for model's validations. For this work, experimental results from Sunliang [66] are used to validate the developed numerical models. The same experimental results have been used to validate the PCM algorithm in EnergyPlus [35]. Fig. 5 shows a schematic diagram of the environmental test chamber, wall configuration and temperature sensor locations across the wall assembly. Table 3 summarizes the material properties used in the validation task. Fig. 6(a) shows the enthalpy-temperature ($h-T$) performance curve for the PCM product used in the experimentation. Fig. 6(b) reports the boundary condition on both sides of the wall. The thermal properties of wall assembly are documented in these references [35,66,67]. The thermocouples have an accuracy of $\pm 0.1^\circ\text{C}$ and the data are recorded at 10 min time intervals.

The numerical models developed for PCMs simulations (refer to Table 2) were exposed to the boundary conditions (refer to Fig. 6(b)) and using the materials properties used in the experiment. Since the experimental results are reported for 10 min, the simulation time step is also similar. Fig. 7(a) and (b) shows the temperature profiles at two points where PCM layer is located (point 2 and 3 in Fig. 5). All models show good agreement with the experimental results except the non-iterative correction scheme proposed by Pham [49]. Although this method is quick, it is inaccurate at 10 min time step. This drawback has been eliminated using the hybrid scheme proposed in this study. Further analysis of the models numerical predictions and errors can be evaluated using methods described by Polly et al. [68]. The root mean squared error (RMSE) is used to evaluate the absolute error between the numerical and experimental results using the following relationship:

$$\text{RMSE} = \sqrt{\frac{\sum_{i=1}^n (\text{prediction} - \text{measurement})_i^2}{n}} \quad (20)$$

Fig. 7(c) shows the RMSE of the models when compared to the experimental results at 10 min time step. All the models, except the non-iterative correction scheme model "EM_NIC_TDMA", show an error close or less than 0.1°C which is within the uncertainty range of the experimental data acquisition equipment.

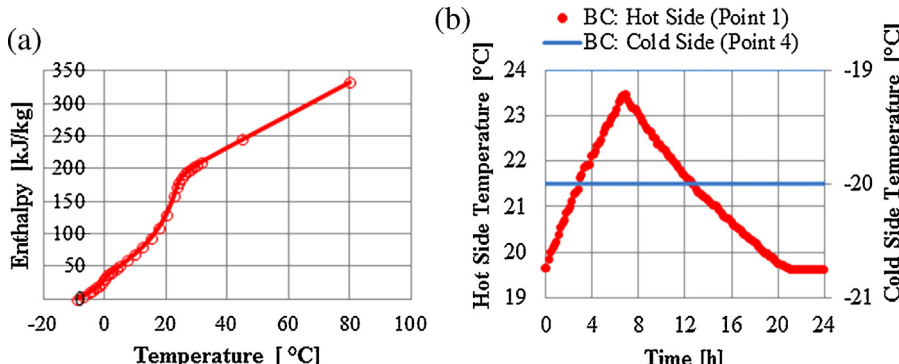


Fig. 6. Thermal characteristics used in the laboratory experiment: (a) PCM's Enthalpy-Temperature performance curve and (b) Boundary conditions.

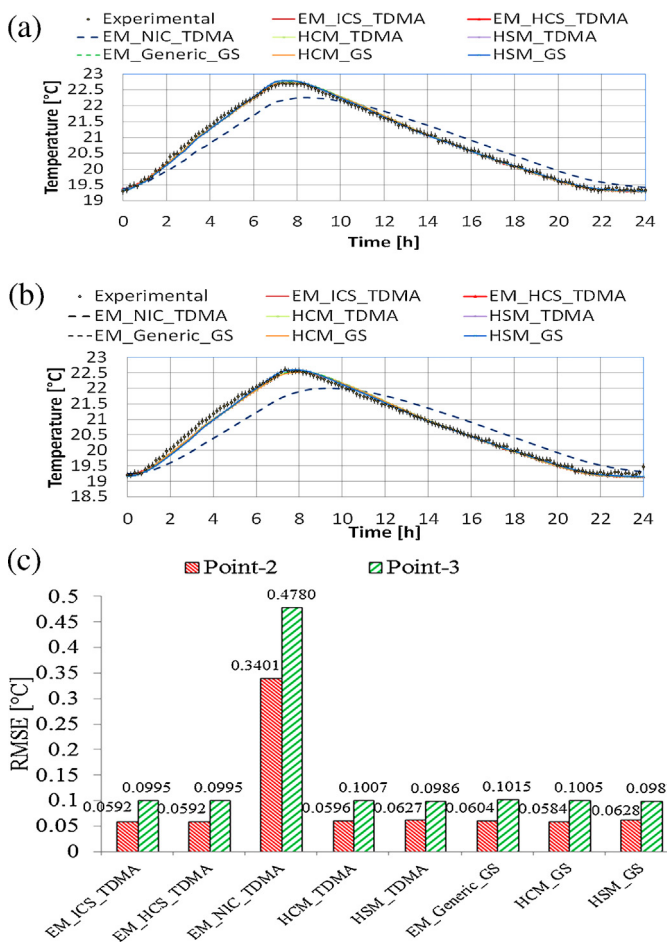


Fig. 7. Validation of numerical models with experimental results, (a) Temperature profile at point 2, (b) Temperature profile at point 3, (c) Root mean squared error for the numerical model's predictions.

3.2. Verification using comparative studies

The experimental validation above does not consider the long wave, short wave radiation, or air convection since temperatures are imposed as boundary conditions on the models. Therefore, a comparative analysis can be used to verify the models when complex boundary conditions are imposed. For this verification, EnergyPlus is used for the benchmark testing. EnergyPlus has recently undergone a rigorous verification and validation process

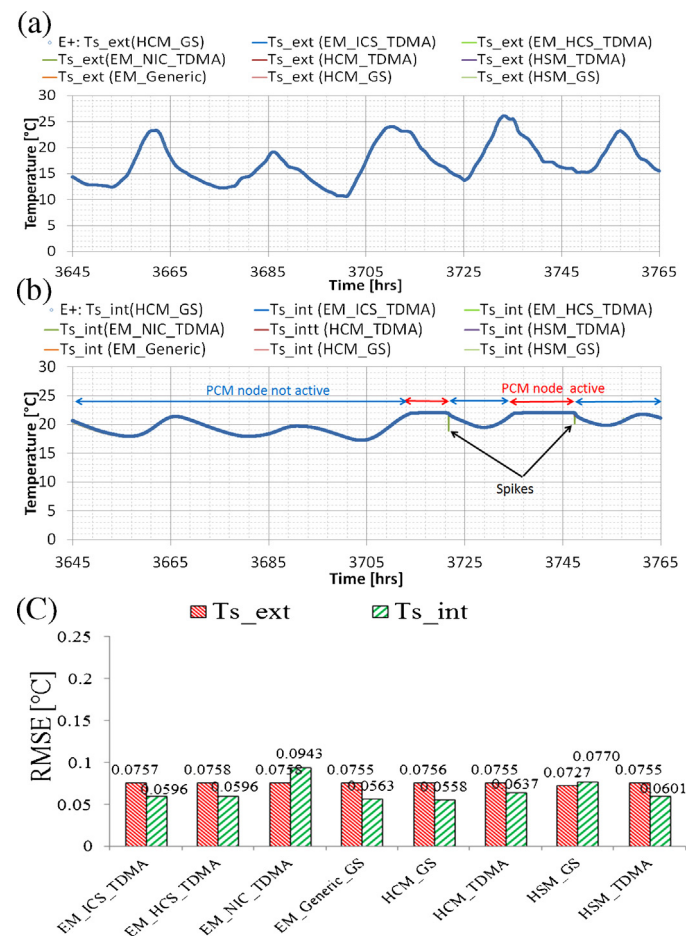


Fig. 8. Verification of the developed numerical models against EnergyPlus for a south wall at 3 min time step: (a) Exterior Surface Temperature, (b) Interior Surface Temperature, (c) RMSE of the numerical models when compared to EnergyPlus results.

[35]. A south wall is assumed to be located in Denver, Colorado. The EnergyPlus weather file for Denver is used to provide the necessary boundary conditions. The results are assumed to converge when error falls below 10^{-7} and maximum iterations allowed are limited to 3000. The material properties and simulation parameters are summarized in Table 4.

Fig. 8 shows the comparison between the developed numerical models and the EnergyPlus results at a time step of 3 min, a maximum time step recommended by the developer for PCM modeling [35]. The exterior and interior surface temperatures are

Table 4

Parameters used for South Wall.

Test parameter	Values			Units
		Concrete (Outside)	PCM (Inside)	
Thermal Conductivity	0.733		0.726	W/m K
Density	2315		1601	kg/m ³
Specific heat capacity	800		836	J/kg K
Thickness	0.15		0.019	m
Latent heat of fusion			13740	J/kg
Melting temperature			22	°C
Melting range			0.10	°C
Mesh grid points	21		21	
Indoor temperature	24			°C
External convective heat transfer coefficient	11			W/m ² K
Internal convective heat transfer coefficient	3.079			W/m ² K
Solar absorption	0.2			
Time step	3 min			
Simulation time	Selected interval where PCM is active and non-active			

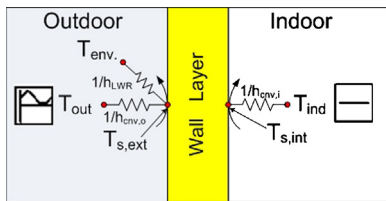


Fig. 9. Illustration of the wall geometry and its boundary conditions.

selected for comparison. The root mean squared error (RMSE) is calculated using Eq. (20). For this calculation, the EnergyPlus results are assumed to be the reference. The calculations are performed over the time interval shown in the figure. It is clear that all models show good agreement with EnergyPlus results for both exterior and interior wall's surface temperatures. The models also show that for the first two days, PCM are not engaged but got engaged when the interior surface temperature reaches 22 °C, which is the melting point of PCM. It is observed that the non-iterative correction scheme (EM_NIC_TDMA) shows temperature spikes for interior surface's node, a node in the PCM layer, and subsequently high errors when PCM node leaves the mushy region. This scheme shows a slightly higher RMSE for nodes with PCM (i.e. interior node) among all models. Generally, the error for all models is less than 0.1 °C for the time step of 3 min as demonstrated in Fig. 8.

4. Sensitivity analysis of numerical models: Comparisons and discussions

Previous sections outlined the calculation procedure for different methods and schemes for simulating PCMs. This section provides a closer insight into the numerical performance of these models to solve the nonlinearity associated with PCMs in conduction-dominated heat transfer case. In particular, the followings are investigated:

- Accuracy and numerical stability:
- Spatial resolution: using grid independent study
- Time resolution: using different time steps
- Computational efficiency: using a normalized CPU time.

4.1. Boundary conditions

This study is based on a simple geometry illustrated in Fig. 9. Both sides of the wall are exposed to a theoretical, yet realistic, boundary conditions considered for building applications.

Table 5 provides detailed assumptions and description of the boundary conditions. The wall is exposed to a fixed air temperature at the indoor side and a sinusoidal periodic steady-state temperature profile on the exterior side. Long wave radiation is assumed to

Table 5

Boundary conditions used for the simulation test cases.

Boundary condition				Unit
Indoor temperature (Tind)	20	°C		
Environmental temperature (Tenv)	Sky Temperature 10	Ground Temperature	Air Temperature	°C
Outside temperature profile (Tout)	Amp [°C] 15	Tout Freq [rad/s] $(2 \times \pi) / (1 \times 24 \times 3600)$	Phase [rad] $(-90 \times \pi) / 180$	Bias [°C] 20
External long-wave radiation heat transfer coefficients (hLWR) [60]				
Sky	$h_{sky} = \sigma \times \varepsilon_w \times F_{sky} \times \beta \times \left(\left((T_{sky} + 273)^4 - (T_{s,ext} + 273)^4 \right) / (T_{sky} - T_{s,ext}) \right)$			W/m ² K
Air	$h_{air} = \sigma \times \varepsilon_w \times F_{sky} \times (1 - \beta) \times \left(\left((T_{amb} + 273)^4 - (T_{s,ext} + 273)^4 \right) / ((T_{amb} - T_{s,ext})) \right)$			W/m ² K
Ground	$h_{ground} = \sigma \times \varepsilon_w \times F_{ground} \frac{(T_{ground} + 273)^4 - (T_{s,ext} + 273)^4}{(T_{ground} - T_{s,ext})}$			W/m ² K
External Convective Heat transfer Coefficient (hcv,o)	29			W/m ² K
Internal Convective Heat transfer Coefficient (hcv,i)	3			W/m ² K

Where: $F_{ground} = 0.5 \times (1 - \cos(surfTilt))$, $F_{sky} = 0.5 \times (1 + \cos(surfTilt))$, $\beta = \sqrt{F_{sky}}$, $\sigma = 5.67e - 8 \text{ Wh/m}^2 \text{ K}^4$

Table 6
Thermal Characteristics of walls used for grid independency.

Test parameter	Sensible wall	Latent wall	Units
	Concrete	PCM	
Thermal conductivity	0.14	0.2	W/m.K
Density	2315	235	Kg/m ³
Specific heat capacity	800	1970	J/kg.K
Thickness	0.05	0.05	m
Latent heat of fusion		300	kJ/kg
melting temperature		23	°C
Melting range		0.1	°C
Initial temperature	20		°C
Grid resolution	Varies: 1, 2, 3, 6	Varies: 1, 2, 3, 6, 12, 24	nodes/cm

be between the exterior surface and the outside environment: sky, ground and air. The outdoor air temperature fluctuates above and below that of the indoor allowing the PCM to charge and discharge during a course of a 24 hour time period. The outdoor air temperature is following a sinusoidal function with assumptions provided in the table below:

$$T_{out}(t) = \text{Amp} \times \sin(\text{Freq} \times t + \text{Phase}) + \text{Bias} \quad (21)$$

4.2. Grid independent study

Grid independent analysis is a crucial step when numerical simulation is used. It is a process of determining a grid resolution at which no improvement is attained when a grid is further refined. The main advantage of performing this task is to save computational time since unnecessary fine grid is eliminated and yet the accuracy is maintained. This task is particularly important when simulating phase change materials due to the high nonlinearity nature of the governing heat transfer equation. It is also valuable when iterative slow solvers are utilized for solving phase change problems. However, grid independent can't be generalized and therefore has to be done for each scheme under study. Therefore, it has been performed for all numerical schemes described above. The temperature profile across the walls is predicted; utilizing a sensible heat storage wall assuming a concrete layer and a latent heat storage wall using a PCM layer. Table 6 summarizes the physical and thermal properties of both cases with various grid resolutions. The grid resolutions for sensible case are 1, 2, 3, 6 nodes/cm. Additional grid points are considered for latent heat case and are 1, 2, 3, 6, 12 and 24 nodes/cm. In addition, 2 boundary nodes are located on wall exterior and interior boundary nodes.

Using the above simulation parameters and assumptions, the results are extracted after the temperature field is stabilized in a sinusoidal steady state. Fig. 10 shows the temperature profile across the concrete and PCM wall under various grid resolutions. Since all numerical models reveal a similar temperature profile

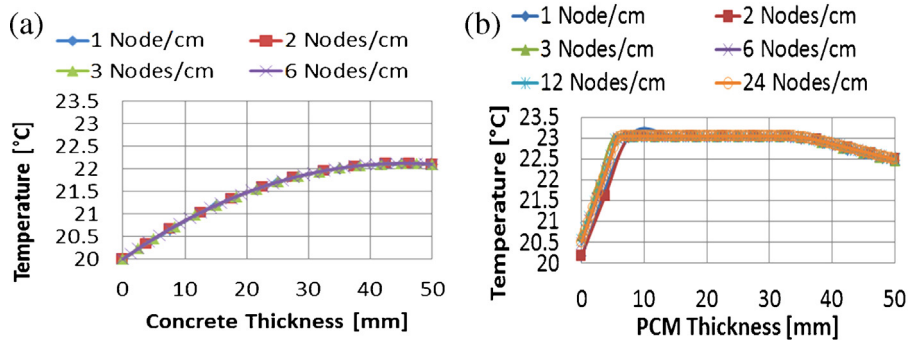


Fig. 10. Grid independent results of the tested models (a) Grid resolution for a 5 cm Concrete wall and (b) Grid resolution for a 5 cm PCM wall.

across the wall, the result of one model is shown in the figure. It is observed that the temperature profile across the concrete wall doesn't improve with increasing the grid resolution. Therefore, 1 node per cm of layer thickness is considered enough for accurate results when considering sensible heat process. However, it is observed that more nodes are necessary when latent heat is considered compared to the sensible case. At least 6 nodes for each cm are necessary for all models. This grid distribution is used in all subsequent analysis.

4.3. Time resolution study

All numerical models use a fully implicit scheme time stepping since it is unconditionally stable regardless of the time step. However, the accuracy will depend on the time resolution. The current state-of-the-art building simulation programs model the building envelopes with or without PCM using a time step of a 1 min (60 s) or more. For the tested cases, a time resolution of 1 min, 5 min, 10 min, 15 min, 30 min, 60 min are considered. It is assumed that the result of each numerical model at a time step of 1 min is the reference case. Therefore, each numerical model is compared to its results at a 1 min time step. Two performance indicators are used to evaluate the results accuracy and the computational efficiency. For accuracy evaluation, the normalized root mean squared error (NRMSE) is adopted using the following relationships [69,70]:

$$\text{RMSE} = \sqrt{\frac{\sum_{i=1}^n (T_{\text{Model}} - T_{\text{Reference}})_i^2}{n}} \quad (22)$$

$$\sigma_{\text{Reference}} = \sqrt{\frac{\sum_{i=1}^n (T_i - \bar{T})^2}{(n-1)}} \quad (23)$$

$$\text{NRMSE}[\%] = \frac{\text{RMSE}}{\sigma_{\text{Reference}}} \times 100 \quad (24)$$

The NRMSE is determined for three nodes; exterior node, interior node and the middle node. The NRMSE is averaged for these three nodes over the simulation time period. The NRMSE value of 100% means that the RMSE is in the bound of the standard deviation [70]. If the errors are higher than these bound values the NRMSE will be above 100%.

The computational efficiency is evaluated using the normalized CPU time (NCPU), using the following equation:

$$\text{NCPU} = \frac{\text{CPU}_{\text{Model}}}{\text{CPU}_{\text{Reference}}} \quad (25)$$

A Quad laptop (Intel i7-2640 M processor, CPU 2.8 GHz, 8G RAM) is used for this analysis. Only one processor is allowed to operate during the simulation and no other tasks, except windows overhead, were running when this task is performed. The CPU time is estimated using a MATLAB benchmarking function "TIMEIT" downloaded from the MATLAB file Exchanger [71]. This code runs each

model three times and averages the CPU times. Two numerical experiments are used in this task:

Case 1: for this case, the melting temperature range is fixed at 0.1 °C and the latent heat of fusion considered are 50, 100, 150, 200 and 300 kJ/kg. This case determines how rigorous the models are when a narrow melting range is assumed. In addition, a latent heat of 0 is used as a benchmark to compare the models when no latent heat is used.

Case 2: for this case, the latent heat of fusion is fixed at 200 kJ/kg and the melting range values are 0.1, 1, 2, and 8 °C. This case determines how sensitive the models are when the melting range varies from a narrow to a wide melting range and the latent heat is fixed.

For both cases, the melting temperature is fixed to 23 °C and a grid resolution of 30 interior nodes and 2 for boundary nodes are assumed as a result of the grid independent study. All simulation parameters and other properties are kept unchanged as per Tables 5 and 6, respectively.

4.3.1. Test Case 1: Varying the latent heat when the melting range is fixed

As noted earlier, each model is compared to itself at a time step of 1 min. The results under this section should not be interpreted as a cross comparison but a self-comparison instead. The models show a similar NRMSE and NCPU pattern and therefore selected results are presented. Fig. 11 shows results of both the NRMSE and the NCPU time for the models under different time steps and varying latent heat. The one minute time step is used as a reference case and therefore not shown in the figure. Fig. 11(a) and (b) shows the performance of the models when no latent heat is modeled. Under this benchmark case, all models show a similar error pattern when the time step increases from 5 min to 60 min. As expected, the error increases as the time step increases since a fully implicit time stepping (1st order approximation) is adopted in this work. The NRMSE for all modes is below 1%. This value will be later used as a threshold NRMSE for the models accuracy when PCMs are used. The NCPU time decreases as the time step increases for all models as shown in Fig. 11(b). Models with iterative solvers (G-S) show high NCPU time reduction when compared to models that uses direct solvers (TDMA). This is not uncommon since direct solvers need less calculation time and therefore low savings on calculation time is expected. At 1 h time step, the iterative solvers take less time to converge when compared to itself at 1 min time step.

For all other latent heat tests, as the time step decreases the NRMSE decreases too as shown in Fig. 11(c), (e), and (g). For some cases, the error is related to the inherited feature of the fully implicit time stepping scheme rather than the models' sensitivity to the latent heat process. This is true for the models that use the correction scheme (EM.ICS_TDMA, EM.HCS_TDMA, HSM_TDMA, and HSM_GS). For these particular models, the NRMSE is between 0.1 and 5% when PCM is used compared to 0.1 and 1% when no PCM

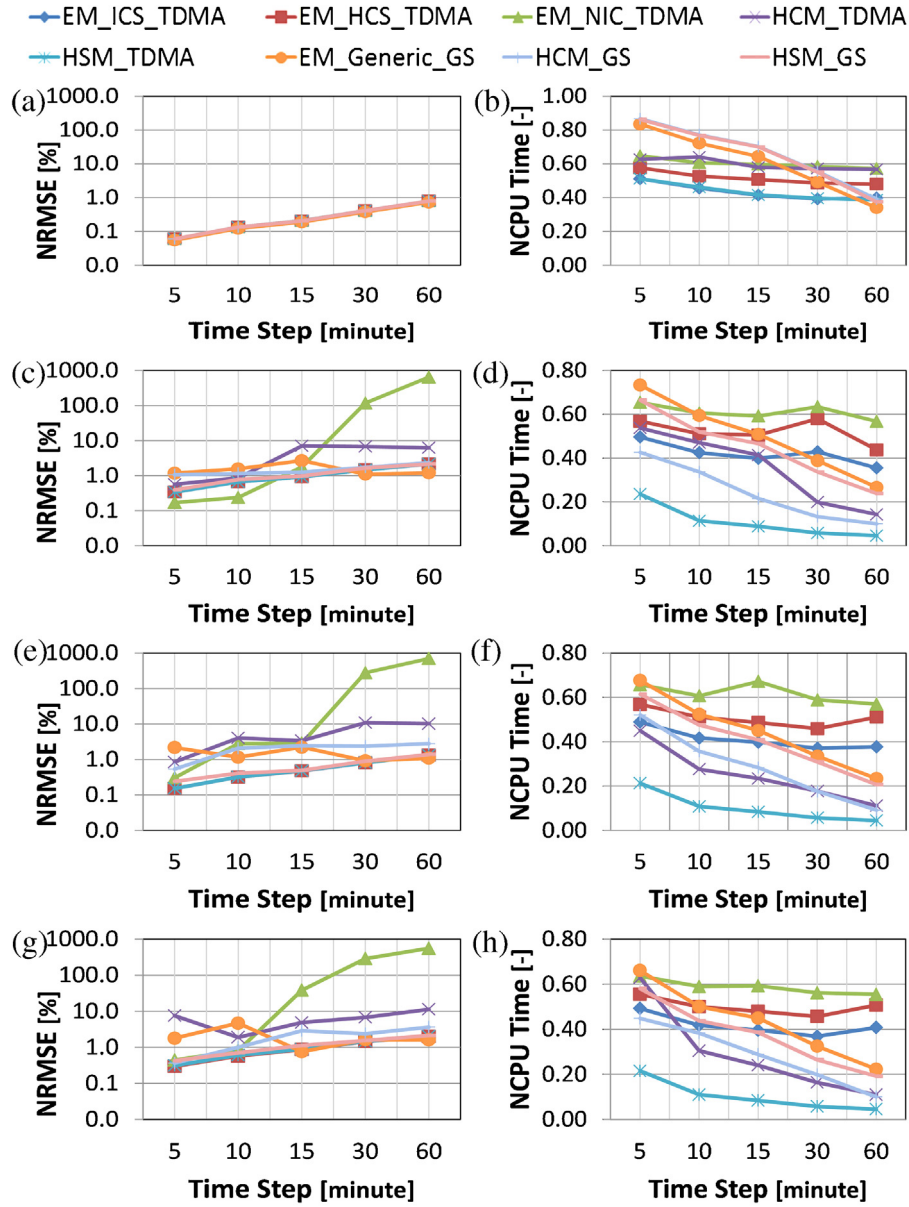


Fig. 11. Performance of different models for various latent heat at fixed melting range of $0.1\text{ }^{\circ}\text{C}$: (a) NRMSE for $L=0\text{ kJ/kg}$, (b) NCPU Time for $L=0\text{ kJ/kg}$, (c) NRMSE for $L=100\text{ kJ/kg}$, (d) NCPU Time for $L=100\text{ kJ/kg}$, (e) NRMSE for $L=200\text{ kJ/kg}$, (f) NCPU Time for $L=200\text{ kJ/kg}$, (g) NRMSE for $L=300\text{ kJ/kg}$, and (h) NCPU Time for $L=300\text{ kJ/kg}$.

is used. The other four models (EM_NIC_TDMA, EM_Generic_GS, HCM_TDMA, and HCM_GS) show higher NRMSE especially at higher time steps due to several reasons. For example, EM_NIC_TDMA model is a semi-implicit since properties are assumed constant based on previous time step. For this method, no further iterations are attempted in a time step which resulted in high errors. Therefore, lower time steps are demanded to reduce the associated NRMSE. The EM_Generic_GS uses under-relaxation factor that has to be optimized for each time step and perhaps for each latent heat case. For this case, however, the under-relaxation factor was fixed and not optimized. Subsequently, the NRMSE is inconsistent across the cases. Heat capacity method (both versions HCM_TDMA and HCM_GS models) occasionally show higher NRMSE (refer to the cases of $L=200$ and 300 kJ/kg). In particular, the HCM_TDMA is not accurate when compared to the HCM_GS even at smaller time step. The heat capacity method uses the numerical approximation for the estimation of the apparent heat capacity. This approximation requires a slow and gradual movement to the solution. This particular requirement can only be achieved using iterative solvers

rather than direct solvers when melting range is very narrow. Since all these variants of Case 1 uses narrow melting range, the TDMA version of heat capacity method is not recommended under this situation.

The NCPU times for the models under different latent heat are shown in Fig. 11(b), (d), (f), and (h). The figure shows the models that use the TDMA with correction scheme do not show major CPU time savings beyond the 5 min time step. It is likely due to small number of iterations at low time steps, consequently lower CPU time. The methods reach convergence quickly regardless of their time step and therefore less CPU savings are achieved. HSM_TDMA (Heat source method, TDMA version) is an exception since it shows a significant CPU time savings when compared to itself at 1 min time step. The methods that implement G-S solvers show a steady decrease in CPU time as the time step decreases. At higher time steps, some methods that use G-S solvers show less NCPU time than those use TDMA. This does not mean that they are quicker than direct solvers, but because they are normalized to themselves at 1 min time step. The NCPU pattern is consistent when increasing

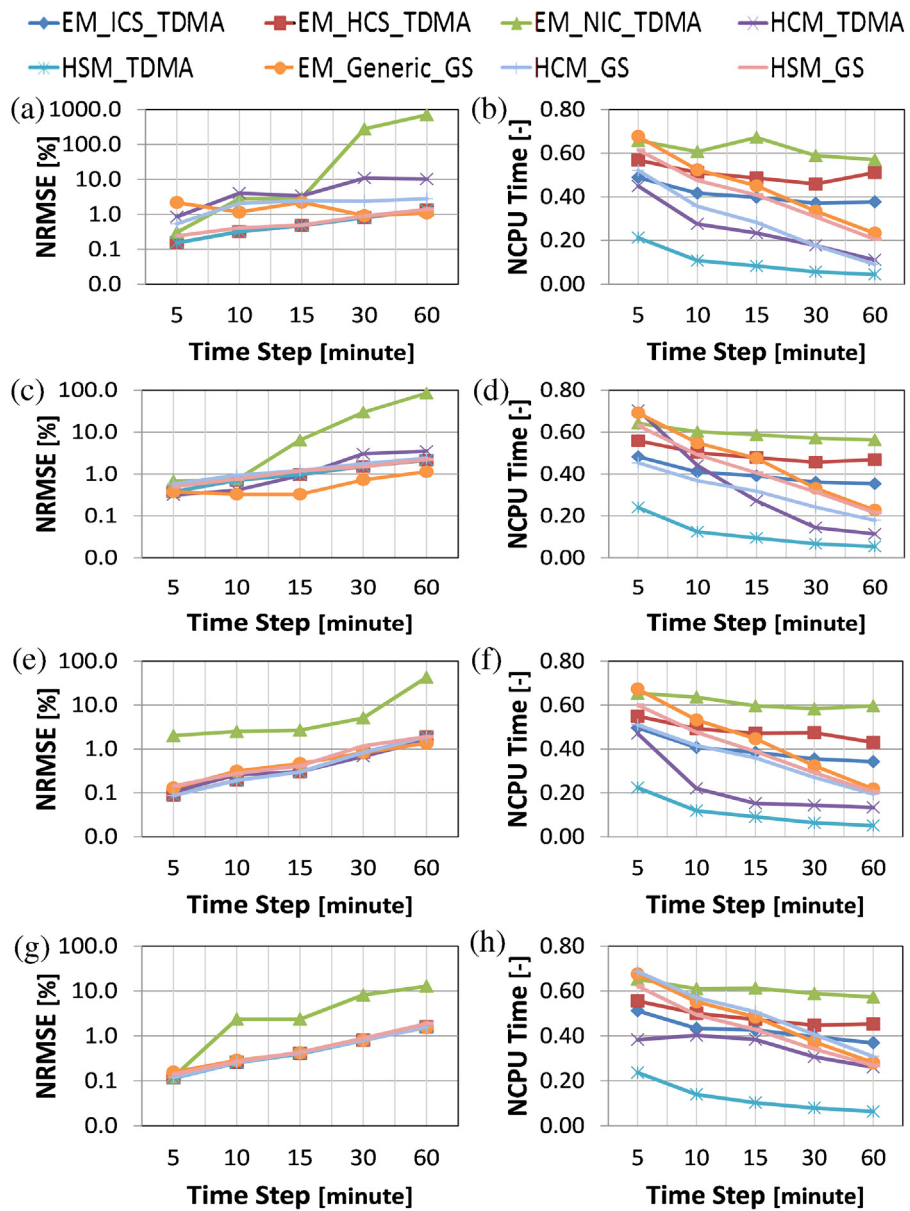


Fig. 12. Performance of the numerical models for various melting range at constant latent heat of 200 kJ/kg: (a) NRMSE for $\Delta T_m = 0.1^\circ\text{C}$, (b) NCPU Time for $\Delta T_m = 0.1^\circ\text{C}$, (c) NRMSE for $\Delta T_m = 1^\circ\text{C}$, (d) NCPU Time for $\Delta T_m = 1^\circ\text{C}$, (e) NRMSE for $\Delta T_m = 2^\circ\text{C}$, (f) NCPU Time for $\Delta T_m = 2^\circ\text{C}$, (g) NRMSE for $\Delta T_m = 8^\circ\text{C}$, and (h) NCPU Time for $\Delta T_m = 8^\circ\text{C}$.

the latent heat and therefore the CPU time is not sensitive to the changes in latent heat.

The overall trend from this case shows that the models are not sensitive to the variations of latent heat since no major improvement or degradation for both the NRMSE and NCPU time are observed. All models show small NRMSE when small time steps are used with an exception of the EM_Generic.GS which is likely related to un-optimized under-relaxation factor. If a threshold of 1% NRMSE is considered (a threshold NRMSE value is based on a sensible case at 1 hour time step), then the models that are based on iterative solvers should be limited to a maximum of 15 min time step. This will result in a significant CPU time savings when compared to a base case of 1 min time step. The Heat capacity method (HCM.GS), however, requires a time step of less than 5 min (refer to Fig. 11(e)). Although high time steps can be used, quick models based on correction scheme (EM.ICS.TDMA, EM.HCS.TDMA, HSM.TDMA, HSM.GS) can be run at 10 or even at 5 min time step without significant CPU overhead.

4.3.2. Test Case 2: Varying melting range with fixed latent heat

This case is intended to evaluate the sensitivities of the numerical methods when the melting range varies from narrow to wide melting range (0.1, 1, 2, and 8 °C) when latent heat is fixed at 200 kJ/kg. Fig. 12(a), (c), (e), and (g) shows that the NRMSE of all models decreases as the melting range becomes wider and eventually converge to the same results. In addition, the models that use the correction scheme (EM.ICS.TDMA, EM.HCS.TDMA, HSM.GS, HSM.TDMA) are less sensitive to the melting range compared to those which don't (HCM.TDMA, HCM.GS, EM.Generic.GS). It is noted that the results from heat capacity method converges to other models as the melting range increases above 1 °C. Since the heat capacity method approximates the slope (i.e. the apparent heat capacity) numerically, the approximation becomes smoother as the melting range is widened and therefore low error is propagated into the calculations. The numerical performance of the EM.NIC.TDMA is not improving for all the cases.

Fig. 12(b), (d), (f), (h) shows that the trend in NCPU time is consistent as the melting range increases. There are no significant

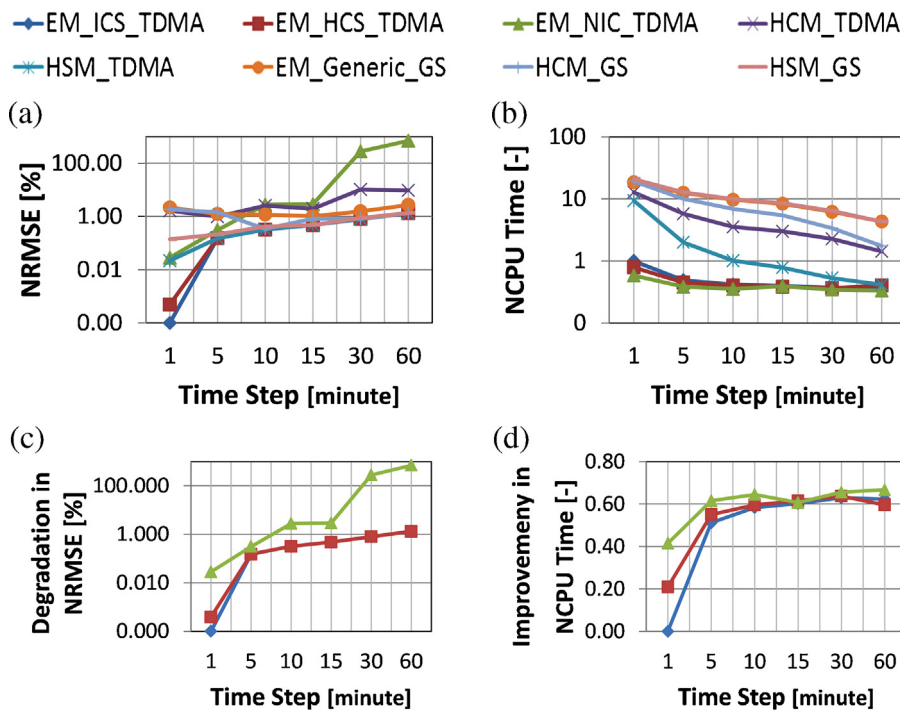


Fig. 13. Cross comparison of different models under narrow melting range at constant latent heat of 200 kJ/kg. (a) NRMSE for $\Delta T_m = 0.1 \text{ } ^\circ\text{C}$, (b) NCPU Time for $\Delta T_m = 0.1 \text{ } ^\circ\text{C}$, (c) Degradation in NRMSE for the quick models, and (d) Improvement in NCPU for the quick model.

changes (improvement or degradation) in NCPU time as the melting range increases for all methods. However, the heat capacity method, specifically the TDMA version, shows inconsistent CPU time as the melting range increases especially for low time steps.

4.3.3. Cross comparison

The previous two cases indicated that there are potential numerical models that could be used for modeling PCM. Models that use correction scheme are found to be less sensitive to the variations of PCM thermal properties; latent heat and melting range. However, the above two cases showed a self-comparison rather than a cross comparison and therefore some important merits are hidden. This section further highlights the accuracy and computational efficiency of these models when one scheme is used as a reference case. The reference case selected for this comparison is the EM.ICS.TDMA. This scheme is found to have

consistent NRMSE and NCPU results all over the analysis. Fig. 13(a) shows the NRMSE of the models when compared to this reference case. The figure shows that there are few models close to the reference case; EM.HCS.TDMA, EM.NIC.TDMA, HSM.TDMA, HSM.GS. These models show a NRMSE of less than 1% at 1 min time step. The EM.HCS.TDMA, hybrid scheme proposed in this study, shows a NRMSE of less than 0.01%. Beyond 5 min time step, these particular schemes have a similar NRMSE as the reference case. Fig. 13(b) shows that enthalpy methods with correction scheme (TDMA versions) are fast although no significant CPU time savings are achieved as the time step increases. All other schemes are at least 10 times slower than these fast schemes at low time steps. The HSM.TDMA shows a significant reduction in NCPU time yet maintaining the same accuracy when compared to other slow schemes. Its computational efficiency is comparable to the fast schemes at 1 hour time step. Since they are the fastest, the enthalpy

Table 7
Summary of sensitivity analysis and recommendation for numerical models for simulating PCMs.

Model	Melting range	Recommended maximum time step [min] [*]	Computational speed	Remarks
Generic Enthalpy Method (EM.Generic.GS)	Becomes accurate with wide melting range ($>1 \text{ } ^\circ\text{C}$)	Inconsistent results at small time steps	Slow	Optimum under-relaxation factor is needed
Iterative Correction Scheme (EM.ICS.TDMA)	Less sensitive to melting range	<15 min	Fast	
Hybrid Correction Scheme (EM.HCS.TDMA)	Less sensitive to melting range	< 15 min	Fast	CPU savings when time step is ≤ 5 minutes
Non-Iterative Correction Scheme (EM.NIC.TDMA)	Inconsistent results	<1 min	Fast	Not recommended since temperature spikes are always there but less severe at low time steps
Heat Capacity Method (HCM.TDMA)	Becomes accurate with wide melting range ($>1 \text{ } ^\circ\text{C}$)	<5 min	Medium	Not recommended since it is highly sensitive to variations in latent heat and melting range
Heat Capacity Method (HCM.GS)	Becomes accurate with wide melting range ($>1 \text{ } ^\circ\text{C}$)	<5 min	Slow	Not recommended since it is highly sensitive to variations in latent heat and melting range
Heat Source Method (HSM.TDMA)	Less sensitive to melting range	<15 min	Medium	
Heat Source Method (HSM.GS)	Less sensitive to melting range	<15 min	Slow	

G-S: Gauss-Seidel, TDMA: Tri-diagonal matrix algorithm.

* This is based on a threshold of 1% NRMSE.

methods with correction scheme are further analyzed as shown in Fig. 13(c) and (d). The figure shows that the EM_HCS_TDMA (hybrid correction scheme) is very close to the EM_ICS_TDMA (iterative correction scheme) which is deemed to be the fast and more conservative [55]. At 1 min time step, the hybrid scheme is 20% faster than the iterative correction scheme. At 5 min time step, the hybrid scheme is 4% faster. There is no significant time savings beyond 5 min time step. The non-iterative correction scheme (i.e. EM_NIC_TDMA) is faster than all of the schemes but has high NRMSE and therefore inaccurate.

4.4. Closing remarks on sensitivity analysis

According to the above results, the numerical schemes have shown to be less sensitive to the variations in latent heat of PCMs. Although some models are associated with high NRMSE, they show consistent NRMSE and NCPU regardless of varying the latent heat. Few models are, however, found to be sensitive to the melting range. In particular, the result from the heat capacity method converges to other schemes when the melting range becomes wider. Models that use correction scheme are found to be less sensitive to the melting range. Further analysis of quick schemes indicated that the hybrid correction scheme (i.e. EM_HCS_TDMA) is faster than the iterative correction scheme's (i.e. EM_ICS_TDMA). This is a significant improvement when a numerical model is sought for building simulation programs that are run for full year simulation at sub-hourly time steps. Table 7 summarizes the findings from the sensitivity study and provides recommendations for selecting a numerical model and scheme for modeling PCM.

5. Conclusions

This study presents the calculation procedure for several numerical models and proposes an improvement to an existing scheme for simulating PCM for implementation into whole building simulation tool. The models have been validated using experimental results from the literature and verified using comparative results from EnergyPlus. All models agree well with both the experimental and comparative results except the linearized enthalpy method with non-iterative correction scheme. The models are then used to perform a sensitivity study on PCM properties; latent heat and melting range at different time steps to evaluate the computational efficiency and the prediction accuracy. The results have given more insights on how the models perform and can be summarized as follows:

- (1) Models that use correction schemes are less sensitive to PCM's latent heat and melting temperature range variations. However, the non-iterative scheme (EM_NIC_TDMA) is found to be less accurate since PCM properties are based on previous time step. If a 1% NRMSE threshold is considered (a maximum NRMSE value achieved with a sensible case at 1 hour time step), the time step could be as maximum as 15 min. However, using a 5 min time step would not add a considerable CPU time. The proposed improvement implemented in the hybrid correction scheme (EM_HCS_TDMA) has resulted in CPU time savings of 20% and 4% at 1 and 5 min time step respectively when compared to the fastest and most conservative scheme; the iterative correction scheme (EM_ICS_TDMA). This improvement is significant when a PCM model is sought for implementation into whole building simulation tool that runs on yearly simulation at sub-hourly time step.
- (2) Direct solver (TDMA) is not recommended for the heat capacity method when PCM exhibits a narrow melting range. Generally, the heat capacity method is found to be sensitive to the

melting range and its prediction converges to the results of other schemes as the melting range increases above 1 °C. This is likely due to the approximation mechanism of the apparent heat capacity, since the sensible and latent heat components are absorbed in this term. The approximation becomes smoother with wide melting range. Therefore, it is recommended that this method is used for PCMs that has a wide melting range, >1 °C. In addition, the time step has to be less than 5 min to achieve a 1% NRMSE threshold value.

- (3) Heat source method, both the TDMA and Guess-Seidel versions, show good predictions when compared to the heat capacity method and comparable results to the linearized enthalpy methods. However, the method is approximately 10 times slower than the linearized enthalpy methods (i.e. the fastest schemes) at small time steps. Although the heat source method uses a correction scheme too, the method utilizes an under-relaxation factor that hindered its speed.
- (4) The general enthalpy method has a similar behavior as the heat capacity method but an optimum relaxation factor is found necessary for accurate results. The method is computationally intensive and doesn't offer an advantage for a potential implementation into building simulation tools.

It is concluded that only two schemes out of eight developed can be considered as potential candidates for integrating into whole building simulation tool; the linearized enthalpy method with the iterative correction scheme (EM_ICS_TDMA) and the hybrid correction scheme (EM_HCS_TDMA). These two schemes offer many advantages over others:

- (1) Flexibility to use with large time steps (a maximum of 15 min) and still with small NRMSE.
- (2) Computational efficiency as they are 3–10 times faster than others based on the time steps.
- (3) Less sensitive to the variation of PCM properties; latent heat and melting range and hence stable in their numerical predictions.

Acknowledgements

This research is part of an ongoing research at University of Colorado Boulder funded by National Science Foundation (EFRI-1038305). The first author would like to thank Sultan Qaboos University for its continuous encouragement and support of research activities.

References

- [1] J.A. Clarke, Energy Simulation in Building Design, 2nd ed., Butterworth-Heinemann, London, 2001.
- [2] X.Q. Li, Y. Chen, J.D. Spitler, D. Fisher, Applicability of calculation methods for conduction transfer function of building constructions, *Int. J. Therm. Sci.* 48 (7) (2009) 1441–1451.
- [3] J. Crank, Free and moving boundary problems, Clarendon Press, Oxford, England, 1984.
- [4] V. Alexiades, A.D. Solomon, Mathematical Modeling of Melting And Freezing Processes, Hemisphere Pub. Corp., Washington, D.C., 1993.
- [5] N. Özisik, Heat Conduction, Wiley, New York, 1993.
- [6] Y. Dutil, D.R. Rousse, N.B. Salah, S. Lassue, L. Zalewski, A review on phase-change materials: mathematical modeling and simulations, *Renewable Sustainable Energy Rev.* 15 (1) (2011) 112–130.
- [7] F. Agyenim, N. Hewitt, P. Eames, M. Smyth, A review of materials, heat transfer and phase change problem formulation for latent heat thermal energy storage systems (LHTESS), *Renewable Sustainable Energy Rev.* 14 (2) (2010) 615–628.
- [8] A. Sharma, V.V. Tyagi, C.R. Chen, D. Buddhi, Review on thermal energy storage with phase change materials and applications, *Renewable Sustainable Energy Rev.* 13 (2) (2009) 318–345.
- [9] P. Verma, Varun, S.K. Singal, Review of mathematical modeling on latent heat thermal energy storage systems using phase-change material, *Renewable Sustainable Energy Rev.* 12 (4) (2008) 999–1031.

- [10] A.F. Regin, S.C. Solanki, J.S. Saini, Heat transfer characteristics of thermal energy storage system using PCM capsules: A review, *Renewable Sustainable Energy Rev.* 12 (9) (2008) 2438–2458.
- [11] B. Zalba, J.M. Marín, L.F. Cabeza, H. Mehling, Review on thermal energy storage with phase change: materials, heat transfer analysis and applications, *Appl. Therm. Eng.* 23 (3) (2003) 251–283.
- [12] S.N. Al-Saadi, Z. Zhai, Modeling phase change materials embedded in building enclosure: A review, *Renewable Sustainable Energy Rev.* 21 (0) (2013) 659–673.
- [13] J.B. Drake, A study of the optimal transition temperature of PCM (phase change material) wallboard for solar energy storage, in, 1987.
- [14] M.J. Huang, P.C. Eames, N.J. Hewitt, The application of a validated numerical model to predict the energy conservation potential of using phase change materials in the fabric of a building, *Sol. Energy Mater. Sol. Cells* 90 (13) (2006) 1951–1960.
- [15] S. Sadasivam, F. Almeida, D. Zhang, A.S. Fung, An iterative enthalpy method to overcome the limitations in ESP-r's PCM solution algorithm, *Anglais* 117 (2) (2011) 100–107.
- [16] F. Almeida, D. Zhang, A.S. Fung, W.H. Leong, Comparison of corrective phase change material algorithm with ESP-r simulation, in: Proceedings of Building Simulation 2011: 12th Conference of International Building Performance Simulation Association, Sydney, 2011.
- [17] C. Chen, H. Guo, Y. Liu, H. Yue, C. Wang, A new kind of phase change material (PCM) for energy-storing wallboard, *Energy Build.* 40 (5) (2008) 882–890.
- [18] A. Pasupathy, R. Velraj, Mathematical modeling and experimental study on building ceiling system incorporating phase change material (PCM) for energy conservation, in: ASME Conference Proceedings, 2006, pp. 59–68, 47837.
- [19] A. Pasupathy, R. Velraj, Effect of double layer phase change material in building roof for year round thermal management, *Energy Build.* 40 (3) (2008) 193–203.
- [20] H. Weinläder, K. Pottler, A. Beck, J. Fricke, Angular-dependent measurements of the thermal radiation of the sky, *High Temp.–High Pressures* 34 (2) (2002) 185–192.
- [21] R.J. Kedl, Conventional Wallboard With Latent Heat Storage For Passive Solar Applications, in: Energy Conversion Engineering Conference, 1990. IECEC-90. Proceedings of the 25th Intersociety, 1990, pp. 222–225.
- [22] J.S. Kim, J. Darkwa, Enhanced performance of laminated PCM wallboard for thermal energy storage in buildings, in: Energy Conversion Engineering Conference, 2002, pp. 647–651.
- [23] K. Darkwa, J.S. Kim, Dynamics of energy storage in phase change drywall systems, *Int. J. Energy Res.* 29 (4) (2005) 335–343.
- [24] A.K. Athienitis, C. Liu, D. Hawes, D. Banu, D. Feldman, Investigation of the thermal performance of a passive solar test-room with wall latent heat storage, *Build. Environ.* 32 (5) (1997) 405–410.
- [25] Z. Ait Hammou, M. Lacroix, A new PCM storage system for managing simultaneously solar and electric energy, *Energy Build.* 38 (3) (2006) 258–265.
- [26] A. Arnault, F. Mathieu-Potvin, L. Gosselin, Internal surfaces including phase change materials for passive optimal shift of solar heat gain, *Int. J. Therm. Sci.* 49 (11) (2010) 2148–2156.
- [27] A. Joulin, Z. Younsi, L. Zalewski, D.R. Rousse, S. Lassue, A numerical study of the melting of phase change material heated from a vertical wall of a rectangular enclosure, *Int. J. Comput. Fluid Dyn.* 23 (7) (2009) 553–566.
- [28] Y. Dutil, D. Rousse, S. Lassue, L. Zalewski, A. Joulin, J. Virgone, F. Kuznik, K. Johannes, J.-P. Dumas, J.-P. Bédécarrats, A. Castell, L.F. Cabeza, Modeling phase change materials behavior in building applications: comments on material characterization and model validation, *Renewable Energy* 61 (0) (2014) 132–135.
- [29] U.S.A. Department of Energy Building Energy Software Tools Directory, URL: (http://apps1.eere.energy.gov/buildings/tools_directory/) [accessed: October/23/2012].
- [30] D.B. Crawley, J.W. Hand, M. Kummert, B.T. Griffith, Contrasting the capabilities of building energy performance simulation programs, *Build. Environ.* 43 (4) (2008) 661–673.
- [31] U.S.A. Department of Energy New Features in Version 2.0.0, URL: (<http://apps1.eere.energy.gov/buildings/energyplus/energyplus.archives.cfm#v4>) [accessed: October/23/2012].
- [32] D. Bradley, M. Kummert, New Evolutions in TRNSYS-A Selection of Version 16 Features, in: Proceedings of Building Simulation 2005: 9th Conference of International Building Performance Simulation Association, Montréal, Canada, 2005.
- [33] University of Strathclyde - Energy Systems Research Unit - ESP-r, URL: (<http://www.esru.strath.ac.uk/Programs/ESP-r.htm>) [accessed: October/23/2012].
- [34] J. Rose, A. Lahme, N.U. Christensen, P. Heiselberg, M. Hansen, Numerical Method for Calculating Latent Heat Storage in Constructions Containing Phase Change Material, in: Building Simulation 2009: 11th International IBPSA Conference, Glasgow, Scotland, 2009.
- [35] P.C. Tabares-Velasco, C. Christensen, M. Bianchi, Verification and validation of EnergyPlus phase change material model for opaque wall assemblies, *Build. Environ.* 54 (0) (2012) 186–196.
- [36] D. Heim, J.A. Clarke, Numerical modelling and thermal simulation of PCM-gypsum composites with ESP-r, *Energy Build.* 36 (8) (2004) 795–805.
- [37] S. Idelsohn, M. Storti, L. Crivelli, Numerical methods in phase-change problems, *Arch. Comput. Meth. Eng.* 1 (1) (1994) 49–74.
- [38] H. Hu, S.A. Argyropoulos, Mathematical modelling of solidification and melting: a review, *Modell. Simul. Mater. Sci. Eng.* 4 (4) (1996) 371–396.
- [39] V.R. Voller, C.R. Swaminathan, B.G. Thomas, Fixed grid techniques for phase change problems: A review, *Int. J. Numer. Methods Eng.* 30 (4) (1990) 875–898.
- [40] V.R. Voller, J.B. Swenson, W. Kim, C. Paola, An enthalpy method for moving boundary problems on the earth's surface, *Int. J. Numer. Methods Heat Fluid Flow* 16 (5) (2006) 641–654.
- [41] N. Shamsundar, E.M. Sparrow, Analysis of multidimensional conduction phase change via the enthalpy model, *J. Heat Transfer* 97 (3) (1975) 333–340.
- [42] C.R. Swaminathan, V.R. Voller, On the enthalpy method, *Int. J. Num. Meth. Heat Fluid Flow* 3 (1993) 233–244.
- [43] E.L. Albasiyy, The solution of non-linear heat-conduction problems on the Pilot Ace, *Proc. IEE, B: Radio Electron. Eng.* 103 (1) (1956) 158–162.
- [44] R.E. White, An enthalpy formulation of the Stefan problem, *SIAM J. Numer. Anal.* 19 (6) (1982) 1129–1157.
- [45] N.R. Eyres, D.R. Hartree, J. Ingham, R. Jackson, R.J. Sargent, J.B. Wagstaff, The calculation of variable heat flow in solids, *Philos. Trans. R. Soc. London, Ser. A: Math. Phys. Sci.* 240 (813) (1946) 1–57.
- [46] C. Bonacina, G. Comini, A. Fasano, M. Primicerio, Numerical solution of phase-change problems, *Int. J. Heat Mass Transfer* 16 (10) (1973) 1825–1832.
- [47] K. Morgan, A numerical analysis of freezing and melting with convection, *Comput. Meth. Appl. Mech. Eng.* 28 (3) (1981) 275–284.
- [48] J.S. Hsiao, B.T.F. Chung, An efficient algorithm for finite element solution to two-dimensional heat transfer with melting and freezing, *J. Heat Transfer* 108 (2) (1986) 462–464.
- [49] Q.T. Pham, A fast, unconditionally stable finite-difference scheme for heat conduction with phase change, *Int. J. Heat Mass Transfer* 28 (11) (1985) 2079–2084.
- [50] A. Faghri, Y. Zhang, Transport phenomena in multiphase systems, Elsevier Academic Press, Amsterdam, 2006.
- [51] X. Zeng, A. Faghri, Temperature-transforming model for binary solid-liquid phase-change problems Part I: Mathematical modeling and numerical methodology, *Numer. Heat Transfer, B: Fundam.* 25 (4) (1994) 467–480.
- [52] X. Zeng, A. Faghri, Temperature-transforming model for binary solid–liquid phase-change problems Part II: Numerical simulation, *Numer. Heat Transfer, B: Fundam.* 25 (4) (1994) 481–500.
- [53] Y. Cao, A. Faghri, C.W. Soon, A numerical analysis of Stefan problems for generalized multi-dimensional phase-change structures using the enthalpy transforming model, *Int. J. Heat Mass Transfer* 32 (7) (1989) 1289–1298.
- [54] V.R. Voller, Implicit finite-difference solutions of the enthalpy formulation of Stefan problems, *IMA J. Numer. Anal.* 5 (2) (1985) 201–214.
- [55] V.R. Voller, Fast Implicit Finite-Difference Method for the Analysis of Phase Change Problems, *Numer. Heat Transfer, B: Fundam.* 17 (2) (1990) 155–169.
- [56] C.R. Swaminathan, V.R. Voller, Towards a general numerical scheme for solidification systems, *Int. J. Heat Mass Transfer* 40 (12) (1997) 2859–2868.
- [57] M. Costa, D. Buddhi, A. Oliva, Numerical simulation of a latent heat thermal energy storage system with enhanced heat conduction, *Energy Convers. Manage.* 39 (3–4) (1998) 319–330.
- [58] M. Salcudean, Z. Abdullah, On the numerical modelling of heat transfer during solidification processes, *Int. J. Numer. Methods Eng.* 25 (2) (1988) 445–473.
- [59] S.V. Patankar, Numerical heat transfer and fluid flow, Hemisphere Pub. Corp., Washington, D.C., 1980.
- [60] U.S.A. Department of Energy - EnergyPlus Engineering Reference, URL: <http://apps1.eere.energy.gov/buildings/energyplus/pdfs/engineeringreference.pdf>. [accessed: October/23/2012].
- [61] N. Shukla, A. Fallahi, J. Kosny, Performance characterization of PCM impregnated gypsum board for building applications, *Energy Procedia* 30 (0) (2012) 370–379.
- [62] C. Ramprasad, L.S. Edwin, F.E. Daniel, An enhanced simulation model for building envelopes with phase change materials, *Anglais* 119 (2) (2013).
- [63] V.R. Voller, An overview of numerical methods for solving phase change problems, in: W.J. Minkowycz, E.M. Sparrow (Eds.), *Advances in numerical heat transfer*, Vol. 1, Taylor & Francis, Washington, D.C., 1997, pp. 341–380.
- [64] K. Morgan, R.W. Lewis, O.C. Zienkiewicz, An improved algorithm for heat conduction problems with phase change, *Int. J. Numer. Methods Eng.* 12 (7) (1978) 1191–1195.
- [65] C. Swaminathan, V. Voller, A general enthalpy method for modeling solidification processes, *Metall. Mater. Trans. B* 23 (5) (1992) 651–664.
- [66] C. Sunliang, State of the Art Thermal Energy Storage Solutions for High Performance Buildings, Department of Physics, University of Jyväskylä, Finland, 2010.
- [67] T. Haavi, M.A. Murphy, F. Kuznik, A. Gustavsen, Zero emission building envelopes—numerical simulations of a well-insulated building with phase change material panels integrated in the floor, in: Proceedings of Building Simulation 2011: 12th International IBPSA Conference, 14–16 November, Sydney, 2011.
- [68] B. Polly, N. Kruis, D. Roberts, Assessing and Improving the Accuracy of Energy Analysis for Residential Buildings (2011), Medium: ED; Size: 41 pp.
- [69] I.H. Witten, E. Frank, Data Mining: Practical Machine Learning Tools and Techniques, Second Edition, Elsevier Science, Amsterdam, 2005.
- [70] G.A.C. Perez, Hybrid Models for Hydrological Forecasting: Integration of Data-Driven and Conceptual Modelling Techniques, CRC Press/Balkema, Delft, the Netherlands, 2009.
- [71] MATLAB File Exchanger, URL: (<http://www.mathworks.com/matlabcentral/fileexchange/18798-timeit-benchmarking-function>) [accessed: November/20/2013].